Proceedings of International Structural Engineering and Construction
Holistic Overview of Structural Design and Construction
Edited by Vacanas, Y., Danezis, C., Singh, A., and Yazdani, S.

ISSN: 2644-108X

PARAPET STIFFNESS EFFECT ON LOAD CARRYING CAPACITY OF MULTI-LANE CONCRETE SLAB BRIDGES

SARAH JABER[1], MOUNIR MABSOUT[1], and KASSIM TARHINI[2]

[1]*Dept of Civil and Environmental Engineering, American University of Beirut, Beirut, Lebanon*
[2]*Dept of Civil Engineering, U. S. Coast Guard Academy, New London, USA*

Bridge specifications do not consider the effect of parapet stiffness in the analysis and design of reinforced concrete slab bridges. This paper performs a parametric investigation using finite element analysis (FEA) to study the effects of parapet stiffness on live load-carrying capacity of two-span, three- and four-lane concrete slab bridges. This study analyzed 96 highway bridge cases with varied parameters such as span-length, bridge width, and parapet stiffness within practical ranges. Reinforced concrete parapets or railings, built integrally with the bridge deck, were placed on one and/or both sides of bridge deck. The longitudinal bending moments calculated using the FEA results were compared with reference bridge cases without parapets, as well as AASHTO Standard and LRFD specifications. The FEA results presented in this paper showed that the presence of concrete parapets reduces the negative bending moments by 15% to 60% and the positive bending moments by 10% to 45%. The reduction in longitudinal bending moments can mean an increase in the load-carrying capacity of such bridges depending on the parapet stiffness. This investigation can assist engineers in modeling the actual bridge geometry more accurately for estimating the load-carrying capacity of existing concrete bridges. Hence, new bridges can be designed by considering the presence of concrete parapets. Parapets can be used as an alternative for strengthening existing one and two-span reinforced concrete slab bridges.

Keywords: Concrete parapets, FEA, AASHTO, LRFD, Span length, Parapet size.

1 INTRODUCTION

In the United States, the majority of highway bridges are short-span, one- and two-span reinforced concrete slabs, prestressed concrete, or steel-girder bridges that are owned and maintained by local governments. These local governments follow the American Association of State Highway and Transportation Officials (AASHTO) Bridge Design Specifications. These specifications may follow the Load Factor Design (AASHTO Standard Specifications (2002)) or the recent probabilistic approach of Load and Resistance Factor Design (AASHTO LRFD Bridge Design Specifications (2012)). The contribution of concrete parapet stiffness is not considered in the load rating of bridges following AASHTO procedures.

Mabsout *et al.* (2004) reported the FEA results of a parametric investigation of simply supported, one-span, concrete slab bridges with no parapets. The results indicated that bending moments calculated using AASHTO Standard Specifications were higher than the FEA moments for one-lane, short-span bridges. The FEA results agreed with AASHTO Standard bending

moments for short-span bridges with two or more lanes. For longer spans, the bending moments calculated using AASHTO Standard Specifications were lower than the FEA moments. However, the AASHTO LRFD procedures overestimated the FEA moments for all bridge cases. In addition, several published studies explored the influence of including the stiffness of concrete parapets and sidewalks of the superstructure and related to the increase in the load-carrying capacity of highway bridges (Mabsout *et al.* 1997, Eamon and Nowak 2005, Chung *et al.* 2006, Conner and Huo 2006, and Akinci *et al.* 2008). Recently, Fawaz *et al.* (2017) reported the influence of adding one standard parapet/railing on increasing the load-carrying capacity of concrete slab bridges. The results indicated that when adding two parapets built integrally with concrete slab bridges, the AASHTO Standard Specifications overestimated the FEA bending moments by 100% for bridge cases with one-lane and 20% for bridge cases with two-lanes. The AASHTO LRFD procedures overestimated the FEA bending moments by 150% for bridge cases with one-lane, and 70% for bridge cases with two-lanes when considering parapets on both sides of the bridge deck. Another recently published study by Jaber *et al.* (2019) presented an investigation of the influence of parapet stiffness on the wheel load distribution as well as the load-carrying capacity in two-span, one-lane, and two-lane concrete slab bridges. Jaber *et al*. (2019) investigated 96 bridge cases that modeled the actual geometry using 3D-FEA. The FEA bending moments due to changes in parapet stiffness compared with reference bridge cases with no parapets as well as with both AASHTO Standard and LRFD design procedures. It was reported that the presence of concrete parapets reduced the FEA negative bending moments by a range of about 55% to 70%. Similarly, the presence of parapets also shows that the FEA positive bending moments reduced by a range of about 40% to 60%. The FEA results demonstrated that accounting for the parapets in the structural analysis could increase the load-carrying capacity of concrete slab bridges by a range of 40% to 70%. This paper builds on and extends the study by Jaber *et al.* (2019) by investigating the influence of parapet size on the load-carrying capacity of two-span, multi-lane, namely three and four lanes reinforced concrete slab bridges.

2 AASHTO BENDING MOMENTS

This investigation uses one of the three procedures suggested by AASHTO Standard Specifications (2002) to estimate the live-load bending moment in concrete slab bridges. The moments calculated using the FEA results were compare to the following AASHTO equations.

$$M = 13{,}500S \ for\ S \le 15m \tag{1}$$

$$M = 1{,}000(19.5S - 90) \ forS > 15m \tag{2}$$

where the longitudinal moment M per unit width is in (N-m/m) and the span length S is in (m).

The AASHTO LRFD Bridge Design Section 4.6.2.3 (2012) uses an equivalent strip width procedure that is comparable to procedures specified in the AASHTO Standard Specifications used in designing concrete slab bridges. The main difference between AASHTO Standard and the AASHTO LRFD is the use of live loading on the bridge. AASHTO Standard Specifications require HS20 truck or lane load and AASHTO LRFD uses HL93 live loading, which combines HS20 Truck with lane loading. This AASHTO LRFD approach consists of calculating the statically designed longitudinal bending moment per unit width.

3 DESCRIPTION OF BRIDGE CASES

This investigation builds on the research reported by Jaber *et al.* (2019) by using typical continuous two-equal-spans and investigating the effect of parapet stiffness on three- and four-

lane reinforced concrete slab bridges. This parametric study considered four typical span lengths of 7.2 m (24 ft), 10.8 m (36 ft), 13.8 m (46 ft), and 16.2 m (54 ft), with slab thicknesses of 450 mm (18 inches), 525 mm (21 inches), 600 mm (24 inches), and 675 mm (27 inches) to control deflection. Bridge widths were 10.8 m (36 ft) for three lanes and 14.4 m (48 ft) for four lanes,

The standard parapet size is adopted from previous research reported by Fawaz *et al.* (2017), assuming rectangular reinforced concrete parapet, that is 200 mm (8 inches) wide and 760 mm (30 inches) high above the deck labeled as X1). The parapets were built as part of the concrete deck. Five different parapet stiffnesses were investigated in this study labeled as X0, X0.5, X1, X2, X3, and X4. Bridge cases with no concrete parapets (X0) assumed as reference cases and used to compare with all bridge cases that considered various parapet stiffnesses. The second moment of area (I) for each parapet was calculated at the base of the cross-section using Eq. (3).

$$I_{(bottom)} = I_{(center)} + Ad^2 = \frac{bh^3}{12} + bh(\frac{h}{2})^2 = \frac{bh^3}{3} \qquad \therefore I_{(bottom)} = 4I_{(center)} \qquad (3)$$

The parapet stiffness had the following second moment of areas such as X0 (I = 0), X0.5 (I = 2Ic), X1 (I = 4Ic), X2 (I = 8Ic), X3 (I = 12Ic), and X4 (I = 16Ic). Figure 1 shows the five parapet sizes (X0.5 through X4) considered in the finite element analysis of 96 bridge cases. Figure 2 shows typical plan-view and cross-section of two-equal-spans (10.8 m or 36 ft each span) for the four-lane bridge case with parapet stiffness (X1). The AASHTO HS20 truck wheel loads positioned longitudinally and transversely to determine the maximum positive moments.

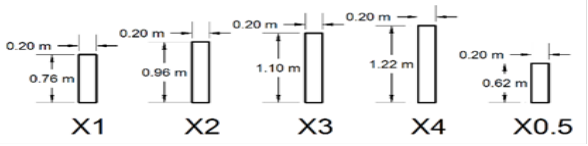

Figure 1. Five Parapet Stiffness Cases (X1, X2, X3, X4, X0.5)

4 BRIDGE LOADING

AASHTO HS20 standard design truck applied on all the bridge cases is formed by using two lines of wheel loads spaced at 6 ft (1.8 m) apart and each line composed of three wheel loads 4, 16, 16 Kips (18 KN, 72 KN, and 72 KN) spaced at 14 ft (4.2 m). These wheel loads placed longitudinally on the bridge deck using influence lines to predict the maximum bending moments in the positive and negative moment regions. The extreme Edge load cases reported by Fawaz *et al.* (2017) adopted in this study. This edge load consists of positioning the center of the left wheel of the left most truck 0.3 m (1 ft) from the left edge of the slab transversely. Additional trucks placed transversely side-by-side with a distance of 1.2 m (4 ft) depending on the number of lanes. This extreme Edge loading is conservative in generating the maximum bending moments in concrete slab bridges. Figure 2 illustrates typical live loading conditions in four-lane bridge cases that identify the critical positive bending moment in two-equal-spans (10.8 m or 36 ft each span).

5 FINITE ELEMENT MODELING

Ninety-six (96) concrete bridge cases considered in this FEA study. The computer structural analysis program SAP2000 (version 19) was used to create 3D-FEA models with four-node SHELL elements for bridge deck and eccentric beam FRAME elements for the parapets (Fawaz *et al.* 2017). Figure 2 shows a typical 3D finite element model of two-equal-spans (10.8 m or 36 ft each span) bridge, four-lanes, and two standard parapets subject to AASHTO HS20 Edge loading condition. Furthermore, Figure 2 shows typical FEA positive moment contours.

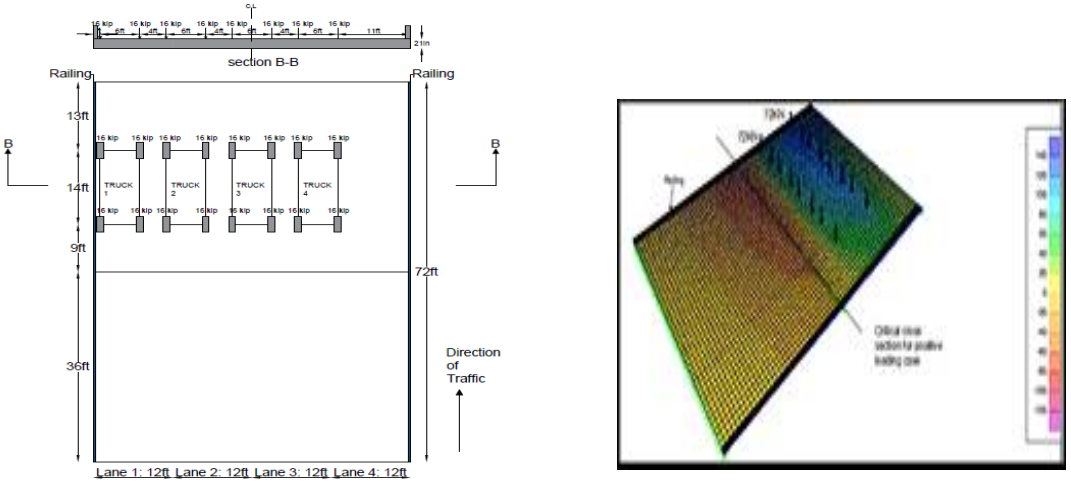

Figure 2. Typical four-lane Edge load case for parapet (X1) and FEA positive moments (KN-m/m).

6 RESULTS OF FINITE ELEMENT ANALYSIS

The 3D-FEA results were presented in terms of the maximum longitudinal bending moments at the critical positive and/or negative cross-sections. These were compared with reference bridge cases with no parapets. The FEA maximum bending moment results were also compared with bending moments calculated using AASHTO Standard and LRFD procedures.

6.1 Comparing FEA Results with AASHTO

The two plots in Figure 3 show the results of FEM longitudinal positive moment at the critical section for all four-lane bridges with parapet stiffness (X1). Figure 3 also shows the FEA positive bending moment plots for all five parapets (X0.5, X1, X2, X3, and X4) for all the four-lane bridge cases as compared to the AASHTO procedures. The first peak bending moment value at the leftmost edge of the critical section is assumed to be resisted by the edge beam. The second peak from the FEA results is assumed to be the maximum bending at the critical section of the slab.

Table 1 summarizes all the maximum FEA positive and negative longitudinal bending moments as compared with the AASHTO procedures. It was observed that, for bridges with no parapets (X0), the AASHTO Standard (2002) procedure generally tends to yield similar results to the FEA negative bending moments. However, for one-lane bridges and span lengths less than 12 m (40 ft), the AASHTO procedures overestimate the FEA negative bending moments by about 20%. This is more pronounced with additional lanes and longer spans, where AASHTO underestimation of the FEA negative moments by 40% for four-lane bridge cases and span lengths greater than 12 m (40 ft). The FEA negative moments decreased significantly for bridges with case parapets (X1) and AASHTO overestimates or gives similar moments in almost all cases, reaching an overestimation of 42% for the three-lane and 36% for four-lane bridges when span lengths are less than 12 m (40 ft). It was noted that as the parapet stiffness increases, the FEA negative moments decrease. The ensuing AASHTO overestimation reached about 65% for three-lane bridges and 40% for four-lane bridges with (X4) parapets.

The AASHTO Standard Specifications generally tend to give similar results to the FEA positive moments for both three-and four-lane bridge cases with no parapets (X0). However, introducing a standard parapet (X1), the FEA positive bending moments decrease significantly as

compared to the over-estimation of AASHTO bending moments. This overestimation of FEA reaches about 28% for the three-lane bridges and decreases to about 16% for four-lane bridges with spans less than 12 m (40 ft). For span lengths longer than 12 m (40 ft), the AASHTO procedures gave similar results to the FEA bending moments after introducing standard parapets. Also, it was noted that as the parapet stiffness increases, the overestimation reached 43% for three-lane bridges and 26% for four-lane bridges with the largest parapet stiffness (X4).

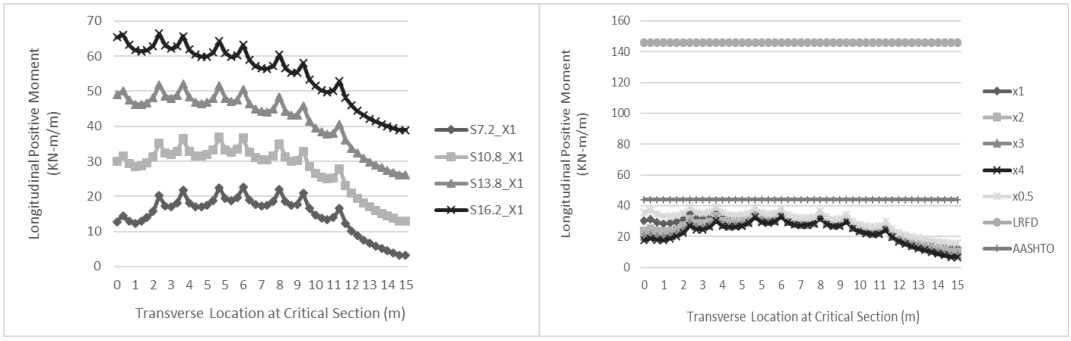

Figure 3. FEA Results of four-lanes with parapet (X1) and AASHTO moments compared with all FEA.

This study showed that the AASHTO LRFD procedure overestimated the FEA moments in almost all the bridge cases with or without parapets. For the three-lane bridge cases, the AASHTO LRFD procedure overestimated the FEA negative moments by 55% and the positive moments by 65%. Similarly, for the four-lane bridge cases, the AASHTO LRFD procedure overestimated the FEA negative bending by 65% and the positive moments by about 72%. When considering parapet cases (X1), the AASHTO LRFD procedure overestimated the FEA bending moments more significantly by reaching an average high of 75% for both negative and positive moments in three- and four-lane bridges, and reached 82% with largest parapet case (X4).

6.2 Influence of Parapet on FEA Results

Table 1 summarizes the FEA maximum positive bending moments for all 48-bridge cases. The bending moments were normalized by taking the ratios of the FEA maximum bending moments for all the bridge cases with parapet stiffness (X0.5, X1, X2, X3, and X4) as compared to the FEA moments for reference bridge cases (X0) without parapets. A similar table was generated for the FEA maximum negative bending moments regions. The presence of parapets reduced the FEA moments and more significantly, as the parapet stiffness increased. For the three-lane bridge cases, the FEA moments reduced by a range of 15% to 20% when adding standard parapets with stiffness factor (X1) and reduced by a range of 20% to 45% when introducing the largest parapet stiffness (X4). However, for the four-lane-bridge cases, the FEA maximum longitudinal bending moments reduced by a range of 10% to 15% when introducing standard parapets with stiffness factor (X1), and reduced by a range of 15% to 35% when introducing the largest parapet stiffness (X4).

7 SUMMARY AND CONCLUSIONS

AASHTO procedures do not account for the presence of parapets when evaluating existing concrete bridges for the load-carrying capacity and when considering permit loads. Based on the results of this study, the presence of parapets can increase deck stiffness and reduce the longitudinal bending moments in the bridge superstructure. Therefore, performing refined 3D-

FEA modeling of existing bridges may help engineers granting permission for over-sized trucks in using specific highway bridge. Bridge engineers can consider adding reinforced concrete parapets as an alternative technique for strengthening or rehabilitating existing bridges.

Table 1. Summary of FEA positive moment with various parapet stiffness.

Number of Lanes	Span Length (m)	Ratio of FEA Maximum Longitudinal Positive Moment with Railings to Reference Case without Railings						Reference Moment X0
		Stiffness Factor						
		X0		X1		X2		
3	7.2	25.2	1.00	21.0	0.83	20.5	0.81	25.2
	10.8	43.1	1.00	33.8	0.78	30.2	0.70	43.1
	13.8	59.5	1.00	50.0	0.84	41.5	0.70	59.5
	16.2	72.8	1.00	62.1	0.85	55.0	0.76	72.8
4	7.2	25.6	1.00	22.6	0.88	22.2	0.87	25.6
	10.8	44.7	1.00	36.9	0.83	34.6	0.77	44.7
	13.8	62.1	1.00	52.1	0.84	47.0	0.76	62.1
	16.2	75.9	1.00	66.4	0.87	59.8	0.79	75.9
		X3		X4		X0.5		
3	7.2	20.2	0.80	20.1	0.80	21.7	0.86	25.2
	10.8	28.3	0.66	27.1	0.63	36.7	0.85	43.1
	13.8	35.9	0.60	32.0	0.54	56.4	0.95	59.5
	16.2	49.9	0.69	46.1	0.63	66.8	0.92	72.8
4	7.2	22.1	0.86	22.1	0.86	22.9	0.89	25.6
	10.8	33.4	0.75	32.5	0.73	38.8	0.87	44.7
	13.8	43.8	0.71	41.4	0.67	55.7	0.90	62.1
	16.2	55.0	0.72	51.2	0.67	70.6	0.93	75.9

Acknowledgments

The authors are indebted and thankful for the generous support and grant from the University Research Board (URB) at the American University of Beirut (AUB), Lebanon.

References

AASHTO, *Standard Specifications for Highway Bridges*, 17th Ed., American Association of State Highway and Transportation Officials (AASHTO), Washington, D. C., 2002.

AASHTO, *LRFD Bridge Design Specifications*, 5th Ed., American Association of State Highway and Transportation Officials (AASHTO), Washington, D. C., 2012.

Akinci, N. O., Liu, J., and Bowman, M. D., *Parapet Strength and Contribution to Live Load Response for Super Load Passages*, Journal of Bridge Engineering, ASCE, 13(1), 55-63, January, 2008.

Chung, W., Liu, J., and Sotelino, E. D., *Influence of Secondary Elements and Deck Cracking on the Lateral Load Distribution of Steel Girder Bridges*, J. of Bridge Engineering, ASCE, 11(2), 178-187, Mar 2006.

Conner, S. and Huo, X. S., *Influence of Parapets and Aspect Ratio on Live-load Distribution.* Journal of Bridge Engineering, ASCE, 11(2), 188-196, March, 2006.

Eamon, C. and Nowak, A*., Effects of Edge-Stiffening Elements and Diaphragms on Bridge Resistance and Load Distribution*, Journal of Bridge Engineering, ASCE, 7(5), 206-214, September, 2005.

Fawaz, G., Waked, M., Mabsout, M., and Tarhini, K., *Influence of Railings on Load Carrying Capacity of Concrete Slab Bridges*, Bridge Structures, IOS Press, 12(3-4), 85-96, June, 2017.

Jaber, S., Mabsout, M., and Tarhini, K., *Influence of Railings Stiffness on Wheel Load Distribution in Two-span Concrete Slab Bridges,* The 10th International Structural Engineering and Construction (ISEC-10*)*, ISEC Society, Chicago, USA, May 20-25, 2019.

Mabsout, M., Tarhini, K., Frederick, G., and Kobrosly, M., Influence of Sidewalks and Railings on Wheel Load Distribution in Steel Girder Highway Bridges, *J. of Bridge Engineering*, 2(3), 88-96, August, 1997.

Mabsout, M., Tarhini, K., Jabakhanji, R., and Awwad, E., Wheel Load Distribution in Simply Supported Concrete Slab Bridges, *Journal of Bridge Engineering*, ASCE, 9(2), 147-155, March, 2004.

SAP2000 (version 19), *Computers and Structures Inc*., Berkeley, California.